Proceedings of the 5th International Conference on Materials Chemistry and Environmental Engineering
DOI: 10.54254/2755-2721/123/2025.19589

Targeted Silver Nanoparticles Loaded with Methotrexate for Rheumatoid Arthritis Therapy

Yixuan Wang[1,a,*]

[1]*Shanghai Qibao Dwight High School, Shanghai, China*
a. yxwang_dorothy@qibaodwight.org
**corresponding author*

Abstract: Rheumatoid arthritis (RA) is a kind of autoimmune disease with a complex pathogenesis, involving immunological, genetic, and environmental factors. Current treatment for RA mainly focuses on alleviating inflammation, and the disease is still hard to be cured completely. Rheumatoid arthritis microenvironment (RAM) makes treatment even more difficult, with synovial hyperplasia, angiogenesis and bone destruction causing RA uncontrollable. Continuous chronic inflammation and retention effect (EPR) of reactive nitrogen and oxygen species (RNOS) in RAM lead to a vicious circle, resulting in difficulty in treatment. In joints of RA, macrophages, especially activated M1 macrophages, produce large amounts of inflammatory cytokines, including TNF-α, IL-1β and IL-6, to maintain and exacerbate joint inflammation. Therefore, M1 macrophages has become an important target to treat RA. This study aims to develop a new treatment strategy by using targeted silver nanoparticles loaded with methotrexate (MTX) and modified folic acid (FA) to achieve M1macrophage targeting. According to previous research articles, modified silver nanoparticles have benign in vitro targeting and treating effects on M1 macrophages, providing a new idea and possibility for RA treatment.

Keywords: Rheumatoid arthritis (RA), Silver nanoparticles (AgNPs), Methotrexate (MTX), Targeted therapy.

1. Introduction

1.1. Research Background

Rheumatoid arthritis (RA) is an autoimmune disease with unknown pathogenesis [1], generally believed to be related to immunological, genetic and environmental factors [2]. More than 20 million people worldwide suffer from this disease each year, with women aged from 35 to 50 being at high risk in China [3]. RA significantly disturbs their daily activities, with severe cases leading to deaths. RA has various characteristics including heterogeneity, systematicness, autoimmunity, and regionality, with clinical manifestation of morning joint stiffness, pain, swelling and severe joint deformity in late stage, and indirectly affects other healthy parts of the body, like lungs [4]. Since the most important pathological feature of RA is continuous chronic inflammation, most therapy nowadays are mainly based on alleviating inflammation influences [5,6]. Specifically, drugs used for treatment at present include non-steroidal anti-inflammatory drugs (NSAIDs), disease-modifying anti-rheumatic drugs (DMARDs), glucocorticoids (GCs), biological agents and traditional Chinese

DOI: 10.54254/2755-2721/123/2025.19589

herbs [7]. In spite of their certain effects on anti-inflammation and alleviation, it is still difficult to cure RA fundamentally with serious side effects of long-term use of drugs [8]. Therefore, further research is required to determine whether other treatments can improve the efficacy of RA treatments.

The incurable progression of RA is caused not only by persistent chronic inflammation, but also by synovial hyperplasia, angiogenesis and bone destruction in RAM [9]. RAM has high permeability and retention effect (EPR), and in RAM unique extracellular matrix molecules that differs from normal cells were observed, including inflammatory factors and reactive nitrogen and oxygen species (RNOS) such as superoxide anion ($O_2^{\cdot-}$), hydrogen peroxide (H_2O_2), hydroxyl radical (OH·), singlet oxygen ($^1O_2$), hypochlorous acid (HOCl), nitric oxide (NO), peroxynitrite ($ONOO^-$), etc [11]. Specifically, vicious circle between RNOS production and inflammatory factors is the main reason why RA is uncontrollable [12]. In joints of RA, the synovial tissue is infiltrated by all types of inflammatory factors, especially macrophages, playing vital roles in pathophysiological reactions. Activated macrophages, also called M1 macrophages, can produce a series of inflammatory factors such as TNF-α, IL-1β and IL-6 to sustain and exacerbate joint inflammation [13]. Therefore, M1 macrophages are considered as a vital target for recurring RA symptoms. For example, different nano carriers have been developed for targeted delivery of methotrexate (MTX) to M1 macrophages. In addition to directly damaging M1 macrophages using MTX, it also fights against other inflammatory diseases by clearing RNOS from RAM. Overall, targeting M1 macrophages to release drugs and clearing RNOS is potentially a promising strategy for RA treatment.

Current nano drug delivery systems for RA treatment can be mainly divided into metal nanomaterials, polymer nanomaterials, vesicae and so on. Among them, the research on metal nanomaterials provides a new idea for the treatment of RA. Some researchers have synthesized cerium-albumin nanoparticles which have peroxidase activity, which can effectively clean RNOS, and are able to transform M1 macrophages into M2 macrophages. The particles have good regulation in balancing RAM and alleviate RA symptoms and have a certain prospect of clinical transformation [15]. Traditional drug therapy cannot treat pathogenic factors at the same time, but nanomaterials can effectively intervene RAM through targeted drug delivery, change its inner structure, and reduce side effects by passive targeting of retention effect, in order to better regulate RAM. Silver nanoparticles (AgNPs) are commercial nanomaterials, which are easy to synthesize and modify, and have wide ranges of biological activities. While acting as a carrier of delivering anti-inflammatory drugs, they also have anti-inflammatory activities, thus adjusting RNOS [16, 17].

Therefore, active targeting of M1 macrophages can be successfully achieved by designing AgNPs as carriers of drug delivery system and modifing them with folic acid (FA). Modified AgNPs (called AgNPs-MTX-PEG-FA) have good targeting and therapeutic effects on M1 macrophages in vitro, proving AgNPs as a possible source of treating RA.

1.2. Research Significance

This research aims to achieve targeted delivery of MTX through AgNPs to improve local treatment effects and reduce systemic side effects. Nanoparticles are promising sources of carriers for drug delivery system in the treatment of RA, and AgNPs showed potential in increasing treatment effects, reducing side effects in patience, and enhancing treatment safety and toleration. Meanwhile, by targeting M1 macrophages, drugs are more accurately delivered to inflamed joint, reducing unnecessary effects on healthy tissues, therefore improving treatment precision. In addition, AgNPs may capable of mediating multiple physiological and pathological effects including anti-inflammation and immunoregulation, providing extra benefits for RA treatment. Furthermore, it is expected to enhance bio-availability of drugs, thus reducing frequency of medication and increasing treatment convenience and compliance in patience. In general, this study hopes to bring more effective and safer choice for RA treatment, in order to help those affected recover as soon as possible.

DOI: 10.54254/2755-2721/123/2025.19589

1.3. Research Purpose

Contraposing the difficulty in RA treatment, low drug utilization and side effect, this experiment aims to solve scientific research questions below through nanoparticles synthesis:

(1) Targeting objective: Whether if this research aims to realize targeting delivery of AgNPs to MTX in order to improve partial accumulation of drugs in RA regions and alleviate non-specific influence in other tissues?

(2) Therapeutic effect objective: Whether if this research evaluates therapeutic effect of targeted AgNPs loaded with MTX to RA treatment, including reduction of joint inflammation factors and clear RNOS?

(3) Side effect reduction objective: Whether if this research tests usage of silver nanoparticles loaded with methoxide helps to reduce systematic side effect and promotes treatment safety? Whether if this research improves bioavailability of methoxide in order to reach site of joint inflammation more effectively and thus reduce mediation frequency?

(4) Anti-inflammation and immunoregulation objective: Whether if this research pays attention to the anti-inflammation and immunoregulation effect carried by silver nanoparticles itself can have potential extra advantages in RA treatment?

2. Materials and Methods

2.1. AgNPs synthesis

AgNPs were synthesized according to reference [18]. Primary steps include: the amount of trisodium citrate, sodium borate and silver nitrate solid needed for making 100 mM trisodium citrate solution, 100 mM sodium borate solution and 10 mM silver nitrate solution was calcualted. The dissolution was enhanced by ultrasound, and 10 mL deionized water was added to dilute each obtained solution Solutions all appeared transparently. After the solutions were prepared, 390 mL deionized water was added to a clean round bottom beaker, then 1.2 mL trisodium citrate solution, 4 mL sodium borate solution and 4 mL silver nitrate solution were added. The mixture immediately turned into pale yellow after adding silver nitrate solution. After that, the beaker was placed on an automatic mixing machine for 30 min in order to ensure complete mixing of different solutions to synthesize AgNPs.

2.2. AgNps-MTX synthesis

First, 10 mg mL^{-1} concentrated MTX solution was prepared . 5 mL dimethyl sulfoxide (DMSO) solution was added in a centrifuge tube, obtaining a colorless pellucid solution. After that 50 mg MTX was weighed using an electric balance and added into the tube, followed by sufficient mixing. The mixture appeared in pale yellow. A syringe was used to extract all the mixture to another centrifuge tube, and then the mixture was injected into the round bottle beaker slowly through rubber plug to make the dripping solution disperse. Fully react with the silver nanoparticles synthesized in II.1 for 3 h. Finally AgNPs-MTX was collected through centrifugation and dispersed in water again. 40 mL solution was added to six 50 mL centrifuge tubes respectively, and the tubes were centrifuged for 15 min at rate of 11000 rpm. The pale yellow supernatant was removed into waste liquid tank and black precipitate was observed at the bottom, which is AgNPs-MTX synthesized. Remaining solution in the round bottom beaker was added in equal volume into 4 centrifuge tubes again, repeat the steps above for 3 times. Finally, black precipitate in 6 tubes was poured into one same tube, which is the final AgNPs-MTX synthesized.

DOI: 10.54254/2755-2721/123/2025.19589

2.3. AgHPs-MTX-PEG-FA synthesis

5 mL synthesized AgNPS-MTX was added into two small glass bottles, which were marked with AgNPs-MTX-mPEG and AgNPs-MTX-PEG-FA respectively for comparison. 0.04 g NH_2-PEG2000-FA and MPEG2000-NH_2 were weighed separately and added into corresponded small bottles. The bottles were placed on a magnetic mixer for 24 h to ensure full mixing of solute and solvent. After reacting for 24 h, two mixtures were respectively devided into 5 equal volume sections and added into 5 clean small centrifuge tubes, followed by a centrifugation for 15 min at speed of 14000 rpm. After the centrifugation, apparent black precipitate and yellow supernatant were observed in each tube. The supernatant was then removed and appropriate amount of deionized water was added. The centrifugation steps were repeated for 3 times until transparent supernatant was observed. Black precipitate in 5 tubes were collected separately and dispersed in 1 mL deionized water. Samples synthesized are experiment group AgNPs-MTX-PEG-FA and comparison group AgNPs-MTX-mPEG.

2.4. Resuscitation and passage of macrophages and human umbilical vein endothelial cells

Take out frozen stored macrophage in cell culture laboratory, with obvious lucid precipitate at the bottom, which indicates the accumulation of macrophages at the bottom at the moment. The frozen cells were thawed in a 37°C water bath for 3-4 min until no distinct precipitated cells were seen, equably mixed in upper cryoprotectant. Around 37.5 mL DMEM culture medium was prepared on a super clean bench as standby, and frozen cells and 3 mL DMEM were injected into a clean centrifuge tube through a pipette, followed by a sufficient mixing. Solution appears in pink. Then liquid in equal volume was prepared for balancing the mixture, centrifuge for 3 min at 1000 rpm. There was an evident gathering of macrophages at the bottom after the centrifugation. The supernatant was removed by an air pump, and around 2 mL fresh culture mixture was added again. After that, 5-6 mL DMEM culture medium and cell suspension from centrifuge tubes were added into a new culture dish. Throw back and force for 6-8 times to make sure that cells and culture medium were fully mixed. Finally, the dish was put into a 5% CO2 incubator at 37°C for culture. Cell resuscitation has completed until now.

RAW264.7 and HUVEC cells were prepared and cultured, and when the cells reached 80-90% confluence, they were washed for 1-2 times using culture medium to remove cell fragments and wastes. Since the two cells were both semi-adherent cells, partial semi-adherent cells can be hit to the bottom using pipette under light reflection. The same is true for other suspended and semi-adherent cells. For adherent cells, due to their strong adhesive power to the culture dishes, they cannot be hit by pipette directly. Pancreatin or other digestive enzymes should be added instead under 37°C to digest the cells. The dishes were appropriately swayed during the process, and 10% fetal calf serum was added as culture medium to stop digestion after reacting for a while. Pipettes were used to blow and hit the adherent cells to better disperse them in culture medium at the bottom. The cell suspension prepared were centrifuged for 3 min at 1000 rpm, and supernatant and cell fragments were removed using an air pump. Around 1 mL fresh culture medium was added, the solution was blown and hit to better mix the cells together with culture medium.The number of cells were then counted. 9 μL solution was taken from 1 mL mixture and added into a new centrifuge tube, then around 5 mL DMEM culture medium was added to dilute the cell solution to 500 times its volume, in order to transplant the cells to 96 pore plate more easily. Finally, pipettes were used to add 100 μL cell solution in every pole. The pore plate was put into an incubator for continuous culturing.

DOI: 10.54254/2755-2721/123/2025.19589

2.5. Cell viability and cytotoxicity test

Different amounts of silver nanoparticles (AgNPs-MTX-PEG-FA and AgNPs-MTX-mPEG) were added into each well with the cultured cell solution to get required concentrations containing 0μM, 25μM, 50μM, 75μM, 150μM, 200μM and 250μM nanoparticles. After that, the plate was put into an incubator for 24 h. After 24 hours of incubation, the plate was taken out and 10μL CCK-8 solution was added to each well, followed by another incubation for 1 h. Finally, the cell viability and cytotoxicity assays of the two celll lines were conducted using ELISA, and the absorbance was read at a wavelength of 450 nm.

2.6. Cell uptake test by flow cytometer

Total RNA Extraction Reagent (R401-01, Vazyme) was used for extracting RNA. HiScript 1st Strand cDNA Synthesis kit (R111-01, Vazyme) was used to synthesize cDNA, which was further used to perform real-time quantitative PCR. cDNA obtained was diluted by reverse transcription using 100 sterile ng μL^{-1} water, and transferred into a 1.5 mL EP tube. The selection of sites on a 96 pore plate was based on sample quantity. Upstream and downstream primers were pre-mixed, and 2 μL of the primer mixture was directly added to the reaction system to a final primer concentration of 10 μM each. 8 μL SYBGreen was added into the system and the plate was subsequently placed on the ice. Next, 1 μL cDNA was added in every pole of reaction tube, ensure it reaches bottom. The 96 pore plate underwent centrifugation at speed of 1000 rpm, and precipitate was observed at pore bottom. LC480 (Roche) was used to conduct quantitative polymerase chain reaction.

2.7. Interleukin and TNF-α levels test

Total RNA Extraction Reagent (R401-01, Vazyme) is used for extracting RNA. Use HiScript 1st Strand cDNA Synthesis kit (R111-01, Vazyme) to synthesize cDNA, and perform real-time quantitative PCR. Dilute cDNA obtained by reverse transcription using 100 sterile ng μL^{-1} water, and transferred into 1.5 mL EP tube. Take a 95 pore plate, design sampling position based on sample quantity. Upstream and downstream primers can be pre-mixed, and directly add 2 μL of the primer mixture to the reaction system when final primer concentration reaches 10 μM. Add 8 μL SYBGreen into the system and place it on the ice. Next, add 1 μL cDNA in every pole of reaction tube, ensure it reaches bottom. The 96 pore plate undergoes centrifuge at speed of 1000 rpm, and insures precipitate to appear at pore bottom. Use LC480 (Roche) to conduct quantitative polymerase chain reaction.

2.8. RNOS clearing ability test

After the cells reached 95% confluence in cell culture dishs, RAW264.7 cells were obtained and centrifuged for 5 minutes. The number of RAW264.7 was counted. After that, RAW264.7 was suspended again and added into 6 culture dishes with a diameter of 3.5 cm at a concentration of 1 mL per pole, cultured in an incubator for 24 hours. 10μL LPS,AgNPs-MTX-PEG-FA, AgNPs-MTX-PEG-FA LPS, AgNPs-MTX-mPEG and AgNPs-MTX-mPEG LPS at a concentration of 10 μM was added in each dish. 6 culture dishes was placed in a 5% CO2 incubator at 37°C for 2 h, and LPS was used to irritate the cells. 5 μM RNOS probe DCFH-DA was used to stain in each dish, followed by another incubation for 20 min. Next, the dishes were for 3 times using PBS to remove excess DCFH-DA outside the cells. Finally, all samples were added into a special sample plate, and scanning laser confocal microscope was used to observe and record the samples.

DOI: 10.54254/2755-2721/123/2025.19589

3. Results and Discussions

3.1. Testing and characteristics of materials

3.1.1. Morphology characterization of AgNPs-MTX-PEG-FA

According to reference, citrate-capped AgNPs is synthesized using $NaBH_4$ as reducing reagent [18]. MTX is loaded on AgNPs surface through electrostatic incorporation, and NH_2-PEG2000-FA was used for further modification. Modify FA on AgNPs surface to make it targeted, and apply NH_2-PEG2000-mPEG as comparison group. Add finally synthesized AgNPs-MTX-PEG-FA solution on ultra-thin copper mesh to form tiny droplets. Put the mesh into TEM for observation. Results are shown in Figure 1. It is clearly seen that the overall shape of AgNPs-MTX-PEG-FA is spherical, with uniform particle size at between 100 nm and 200 nm. Additionally, AgNPs-MTX-PEG-FA can be easily dispersed in water solution.

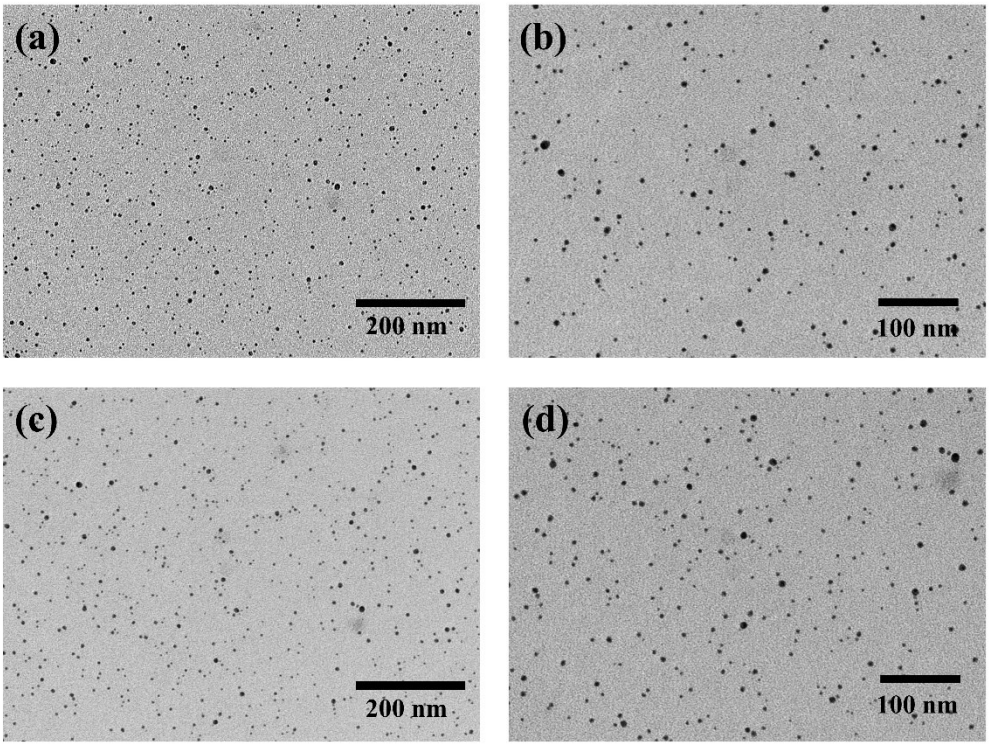

Figure 1: (a)(b) TEM image of AgNPs-MTX-mPEGTEM; (c)(d) TEM image of AgNPs-MTX-PEG-FA.

3.1.2. Property characterization of AgNPs-MTX-PEG-FA

The average hydrated particle sizes of AgNps-MTX-mPEG and AgNPs-MTX-PEG-FA were 86.59 nm and 149.63 nm, respectively. AgNPs-MTX-PEG-FA presented bigger hydrated particle sizes, which may due to FA modification leaded to wider particle size distributions. Also, FA modified particles showed increased water solubility, and a consistent trend was observed for the corresponding PDI value of AgNPs-MTX-PEG-FA. The PDI value of AgNPs-MTX-PEG-FA was around 0.30, showing an enhanced dispersibility. Zeta potential measurements showed that the zeta potential of AgNps-MTX-mPEG and AgNPs-MTX-PEG-FA were -1.70 mV and -6.27 mV, respectively. The change of zeta potential may be due to the replacement of negatively charged citrate to FA on the surface of AgNPs.

DOI: 10.54254/2755-2721/123/2025.19589

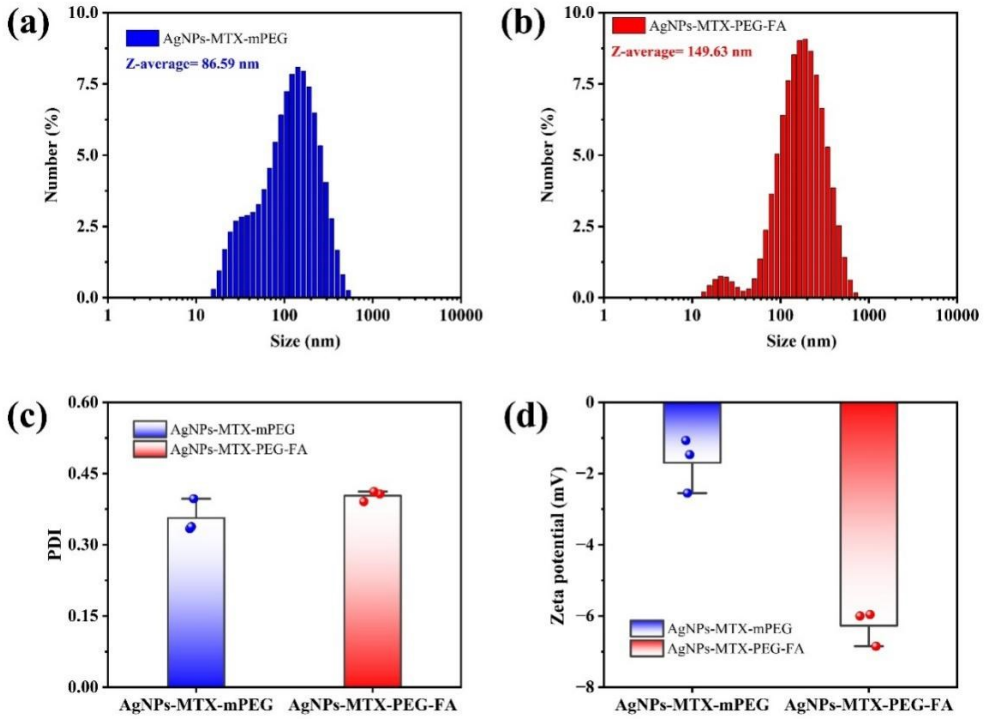

Figure 2: (a) Hydrated particle size of AgNPs-MTX-mPEG and (b) AgNPs-MTX-PEG-FA; (c) PDI value; (d) Zeta potential.

3.1.3. Structural characterization of AgNPs-MTX-PEG-FA

UV absorption peaks of AgNPs-MTX, AgNPs-MTX-mPEG and AgNPs-MTX-PEG-FA were all observed at around 400 nm wavelength. Meanwhile, strong UV absorption peaks were also observed at around 200 nm wavelength, which indicated MTX was successfully loaded on the surface of AgNPs. For AgNPs-MTX-PEG-FA, another absoprtion peak was observed at 600 nm wavelength, which indicated FA was successfully connected onto AgNPs surface (fig.3a). A consistent pattern was observed for the corresponding transmittance of AgNPs-MTX-PEG-FA (fig.3b).

AgNPs-MTX-PEG-FA shows characteristic absorbance vibration at 845-945 cm^{-1} (which may be stretching motion of N-H in FA), 1480 cm^{-1} (absroption band of benzene in FA), and ~1650 cm^{-1} (amido bond in FA and H-N-C=O flexural vibration) [19].

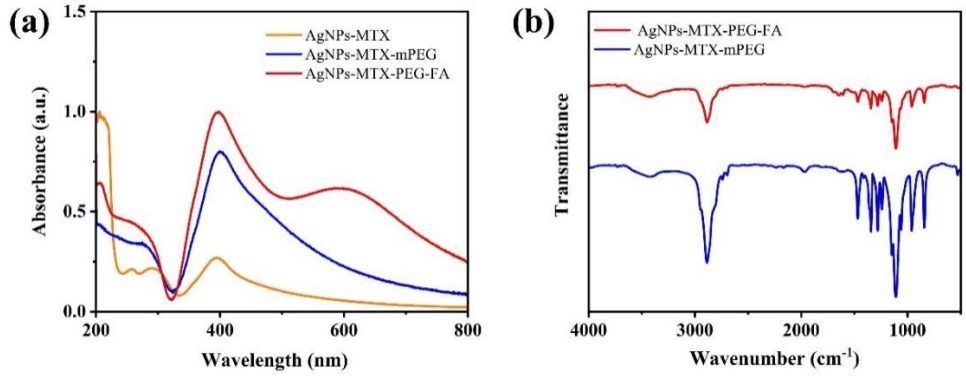

Figure 3: AgNPs-MTX-mPEG and AgNPs-MTX-PEG-FA (a) ultraviolet absorption spectrum; (b)infrared spectroscopy.

DOI: 10.54254/2755-2721/123/2025.19589

3.1.4. Drug release testing of AgNPs-MTX-PEG-FA

The drug loading rates of AgNPs-MTX-mPEG and AgNPs-MTX-PEG-FA were further tested. First, the calibration curve of MTX was drawn, and the linear-regression equation of the curve for MTX was y=14.64236x+0.03009 (R^2=0.9963). Both of the particles were respectively reacted with 1 mM H_2O_2, and large number of bubbles and heat were released, proving that AgNPs-MTX-PEG-FA had the ability to release RNOS responsiveness. At the same time, both solutions turned from yellow to white. After the reaction, both solutions were diluted and their ultraviolet absorption were 0.17267 and 0.14634. After calculation, the drug loading rates of AgNPs-MTX-mPEG and AgNPs-MTX-PEG-FA were 58.2% and 44.4%, respectively. The drug loading rate of AgNPs-MTX-PEG-FA was lower than that of AgNPs-MTX-mPEG, which may be caused by good water solubility brought by folic acid during synthesis, leading to greater amount of MTX been washed during centrifugation, resulting in low drug loading rate. which may be due to FA modification increased the water solubility of the particles, leading to more MTX was washed away during centrifugation.

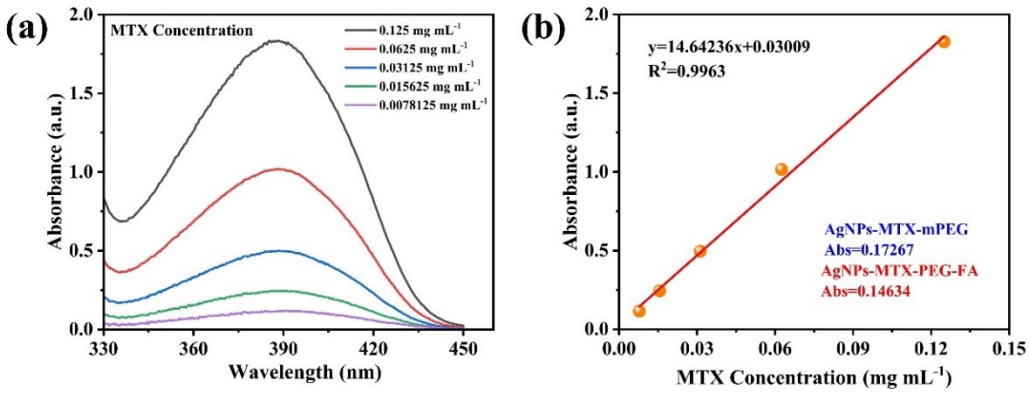

Figure 4: (a)Ultraviolet absorption spectrum of MTX with different concentrations; (b)MTX concentration fitting curve.

3.2. In vitro characterization testing of materials

3.2.1. In vitro cytotoxicity test

The cell counting kit-8 (CCK-8) was used to measure the cytotoxicity of AgNPs-MTX-PEG-FA, and AgNPs-MTX-mPEG was used as the comparison group. The experiment results showed that effects of AgNPs-MTX-PEG-FA on cell viability was negligible. In HUVEC cells, cell viability decreases slightly in higher concentration. It is worth noting that even in the highest concentration (300 μM), cell viability remains above 75%, indicating low toxicity of both material on HUVEC cells. A similar trend was also observed in RAW264.7 cells. However, in RAW264.7 cells, when concentration of AgNPs-MTX-PEG-FA applied was higher than 100 μM, cell viability decreased to less than 75%, even lower than the cell viability of HUVEC cells treated with the highest concentration (300 μM) of AgNPs-MTX-PEG-FA. This could be caused by strong toxicity of released silver ions. In all groups, cell viability rates at concentration of 50 μM were highest, therefore, concentration of 50 μM was used for further RNOS clearing assay. An concentration dependent toxicity of AgNPs-MTX-PEG-FA on LPS-activated RAW264.7 cells was observed, possibly because of the increased toxicity in partially decomposed material caused by AgNPs-MTX-PEG-FA targeted RAW264.7 cell. In all, these observations all showed AgNPs-MTX-mPEG and AgNPs-MTX-PEG-FA were safe biocompatible materials.

DOI: 10.54254/2755-2721/123/2025.19589

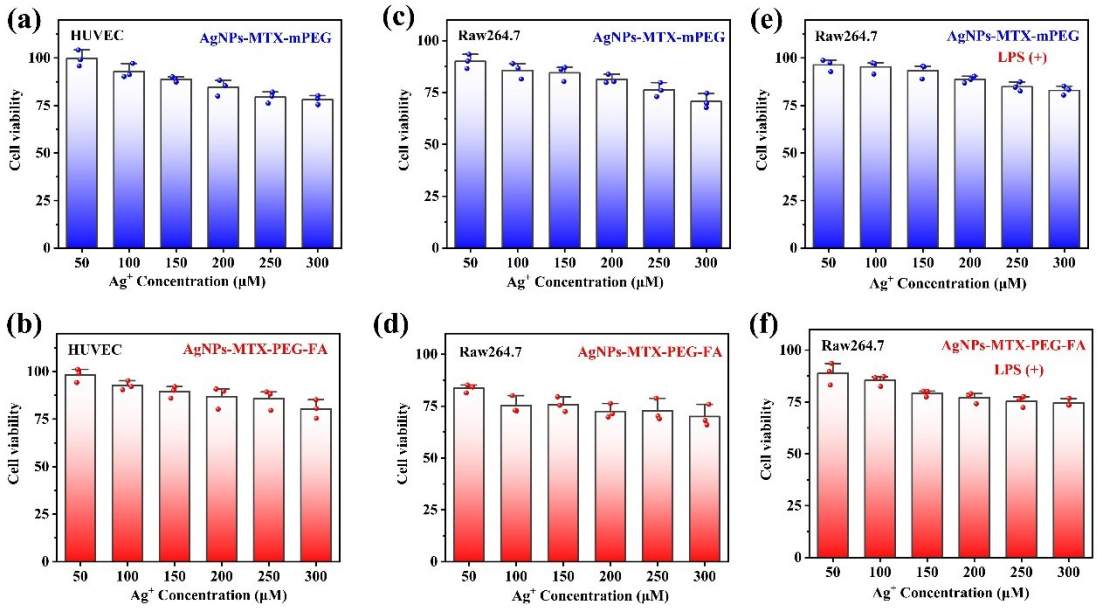

Figure 5: AgNPs-MTX-mPEG and AgNPs-MTX-PEG-FA under different concentration with cells cultured after 48 h, in vitro cytotoxicity test of (a)(b)HUVEC cells, (c)(d)RAW264.7 cells, and (e)(f)activated RAW264.7.

3.2.2. In vitro cell uptake

In order to track AgNPs-MTX-PEG-FA inside cells, FITC fluorophores were used to label the particles, and cell positions were located based on DAPI-stained nucleus. After culturing for 2 h, activated RAW264.7 cells showed green fluorescence, indicating efficient cellular uptake of AgNPs-MTX-PEG-FA (Figure 6). The specific uptake was attributed to overexpression of folate receptor β on activated RAW264.7 cells. However, green fluorescence could also be observed in some inactivated cells, which might be due to the non-specific cellular uptake of AgNPs-MTX-PEG-FA.

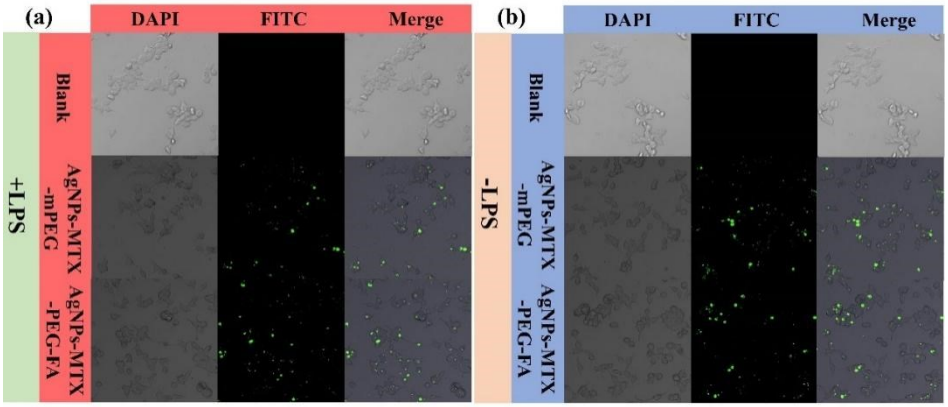

Figure 6: Fluorescent confocal images of FITC labeled AgNPs-MTX-mPEG and AgNPs-MTX-PEG-FA with (a)activated RAW264.7 cell and (b)RAW264.7 cell after culturing for 2 h.

Flow cytometry analysis was conducted for characterization of AgNPs-MTX-mPEG and AgNPs-MTX-PEG-FA. Activated RAW264.7 cells treated with AgNPs-MTX-PEG-FA showed stronger florescence than normal RAW264.7 treated with same particles (fig.7), proving the existence of cell-specific targeting. On the other hand, there is slight difference in fluorescence intensity between

DOI: 10.54254/2755-2721/123/2025.19589

AgNPs-MTX-mPEG and AgNPs-MTX-PEG-FA, and the flow cytometer result is consistent with the fluorescence microscope result.

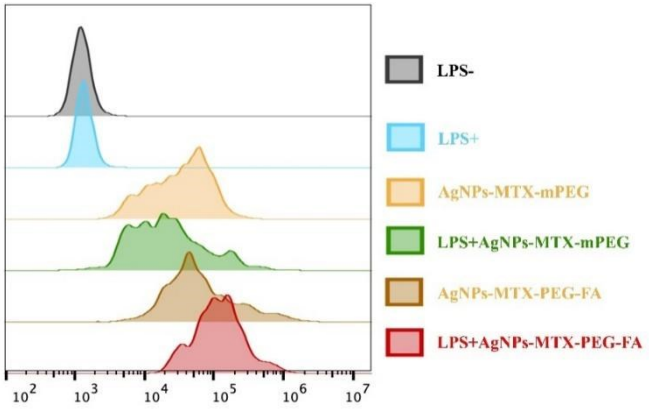

Figure 7: Flow cytometer images of FITC labeled AgNPs-MTX-mPEG and AgNPs-MTX-PEG-FA with activated RAW264.7 cell and RAW264.7 cell after culturing for 2 h.

3.2.3. RNOS clearing capability

Oxidative stress means intracellular antioxidant imbalance caused by production of RNOS, resulting in a series of cell function disability. In order to study RNOS clearing capability of AgNPs-MTX-PEG-FA in activated macrophages, 2'-7'-DCFH-DA probe was used to detect overall RNOS level in cells. After spreading into cells, DCFH-DA probe was transferred into DCFH by cell esterase deacetylation and further oxidised by RNOS, producing green fluorescence DCF for detecting ROS. In inactivated cells, no obvious fluoscence was detected, showing the level of ROS produced was low. In LPS-activated cells, the RNOS production was significantly increased, resulting in a high level of ROS and bright fluorescence. However, in RAW264.7 cells treated withAgNPs-MTX-mPEG or AgNPs-MTX-PEG-FA, the bright fluorescence was not observed, indicating the levels of RNOS were greatly lower. The fluorescence intensity results showed that AgNPs-MTX-PEG-FA had the most obvious effect on clearing RNOS, proving that AgNPs-MTX-PEG-FA has strong RNOS scavenging activity and good therapeutic potential for treating RA. AgNPs-MTX-PEG-FA can improve the vicious cycle between RNOS and M1 macrophages and suppress inflammation, and thus alleviate RA-related symptoms. Overall, AgNPs-MTX-PEG-FA was expected to become a new pharmaceutical nanocarrier in treating RNOS-related diseases, and has wide prospect applications.

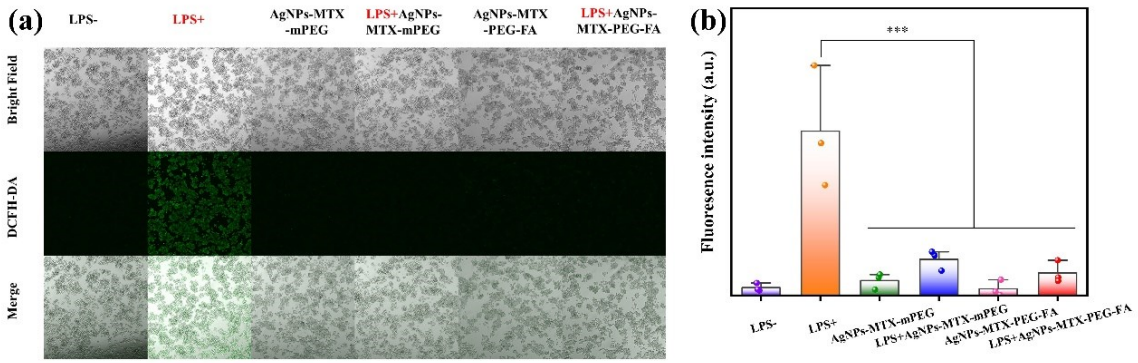

Figure 8: (a)Fluorescent images of cells stained by RNOS fluorescent probe DCFH-DA after different treating; (b)Fluorescence intensity quantification.

DOI: 10.54254/2755-2721/123/2025.19589

3.2.4. Inflammatory cytokines reduction

RAW264.7, a macrophage cell line, has two main functionally phenotypic states, which are M1 and M2 phenotypes. In RA joints, RAW264.7 mainly presents the proinflammatory M1 phenotype, which promotes the progression of RA through pro-inflammatory cytokine production [22]. Therefore,conversion of M1 macrophages into M2 macrophages is a potential method to treat RA. Macropahge markers (including TNF-α and IL-1β) were measured by qPCR analysis. From Figure 9, activated RAW264.7 treated with AgNPs-MTX-PEG-FA showed significant decrease in expression levels of inflammatory cytokines TNF-α and IL-1β. The expression levels of inflammatory cytokines TNF-α and IL-1β decreased by 8 times in activated RAW264.7 treated with AgNPs-MTX-PEG-FA compared to those levels in normal activated RAW264.7.

In conclusion, reduction of inflammatory cytokines indicated that AgNPs-MTX-PEG-FA had an inhibitory effect on inflammation. AgNPs-MTX-PEG-FA could alter macrophage polarization and thus regulate the expression of inflammatory cytokines to exert anti-inflammation activity, which could alleviate inflammation-associated symptoms of RA.

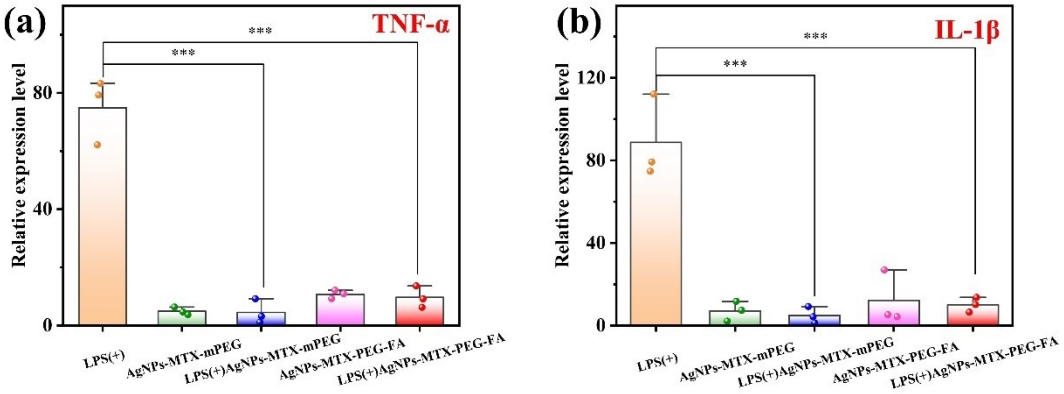

Figure 9: Expression level of inflammatory cytokines in activated RAW264.7 after different treatment (a)TNF-α and (b)IL-1β.

4. Conclusion and Evaluation

4.1. Summary of experimental results

In conclusion, this experiment aims to explore a new treatment strategy, which is using AgNPs loaded with MTX for RA treatment. RA is an autoimmune disease, which has a pathogenesis involving different factors, resulting in joint inflammation, deformities and other health problems. Traditional treatment mainly focuses on alleviating inflammation, but hard to achieve complete cure. In addition, long-term use of drugs can possibly be associated with serious side effects. By designing AgNPs loaded with MTX to realize M1 macrophage targeting, we propose a new treating method. Through our study, modified AgNPs showed good potential in targeting and M1 macrophages *in vitro*. This approach has a big advantage of precise intervention to the inflammation site through nanoparticle-based drug delivery systems, which reduces side effects in traditional approaches. The application of targeted silver nanoparticles not only effectively transfers MTX to key inflammation regions, but also has its own anti-inflammatory activity, bringing double benefits for RA treatment.

DOI: 10.54254/2755-2721/123/2025.19589

4.2. Limitation analysis

Though targeted silver nanoparticles loaded with methotrexate for rheumatoid arthritis therapy proposes a promising therapeutic strategy, some possible limitations are still remained:

Laboratory validation limitations: Recent studies mainly focuses on in vitro experiments, but lack of enough in vivo experiment proof. Although good results have been achieved at cellular level, the actual effect on animal model and human needs further verification.

Drug release efficiency: Although targeted AgNPs is designed to transfer MTX, its drug release efficiency still remains a problem. The effectiveness of drug release needs regulation of various factors, including particle stability and in vivo environment, which could affect actual treatment effect.

Long-term safety: The long-term safety of AgNPs remains an unknown factor. AgNPs can possibly cause potential toxicity effect on human, and thus needs further toxicological studies to ensure safety during treatment process.

Take all these limitations into account, further researches are needed to further explore the feasibility and practically of this method, and focuses on a comprehensive evaluation of its safety and clinical efficacy.

4.3. Future study

Targeted silver nanoparticles loaded with methotrexate for rheumatoid arthritis therapy shows strong treating potential, and may lead the development of RA therapy. Benifits listed below are what this therapy strategy might bring in the future:

Accurate treatment: Targeted AgNPs enables precise delivery of MTX to realize local treatment in key inflammation joints. This accurate treatment is expected to reduce unnecessary harm in healthy tissues and thus improves treating effects.

Reduction of side effects: Through local treatment and accurate delivery, this treating strategy hopes to alleviate systematic side effect caused by long-term use of drugs for patients. This has significant implication for improving treatment safety and tolerability.

Individualized treatment: The treatment strategy of AgNPs loaded with MTX can possibly provide more individualized treatment for patients. More accurate treatment method can be designed based on patient's physiological status and immune characteristics.

Multimodal therapy: Future study can probably combine AgNPs loaded with MTX with other treating methods to realize multimodal therapy. Such treating system can more comprehensively intervene multiple pathological processes of RA and improves overall treating effects.

In conclusion, targeted silver nanoparticles loaded with methotrexate brings new hope for rheumatoid arthritis therapy. Future studies and clinical practices will further reveal its advantages and potential clinical prospect applications for RA therapy, and are expected to make important contributions in improving life quality and treating effects for patients.

References

[1] *Weyand, C. M.; Goronzy, J. J., The immunology of rheumatoid arthritis. Nature Immunology 2021, 22 (1), 10-18.*
[2] *Ding, Q.; Hu, W.; Wang, R.; Yang, Q. Y.; Zhu, M. L.; Li, M.; Cai, J. H.; Rose, P.; Mao, J. C.; Zhu, Y. Z., Signaling pathways in rheumatoid arthritis: implications for targeted therapy. Signal Transduction and Targeted Therapy 2023, 8 (1), 68.*
[3] *Radu, A. F.; Bungau, S. G., Management of rheumatoid arthritis: An overview. Cells 2021, 10 (11), 2857.*
[4] *Kim, J. M.; Kim, H. Y., Pathogenesis of rheumatoid arthritis. Journal of the Korean Medical Association 2010, 53 (10), 853-861.*
[5] *Coutant, F.; Miossec, P., Evolving concepts of the pathogenesis of rheumatoid arthritis with focus on the early and late stages. Current Opinion in Rheumatology 2020, 32 (1), 57-63.*

DOI: 10.54254/2755-2721/123/2025.19589

[6] Finckh, A.; Gilbert, B.; Hodkinson, B.; Bae, S. C.; Thomas, R.; Deane, K. D.; Alpizar-Rodriguez, D.; Lauper, K., Global epidemiology of rheumatoid arthritis. Nature Reviews Rheumatology 2022, 18 (10), 591-602.

[7] Wang, Y.; Chen, S. J.; Du, K. Z.; Liang, C. X.; Wang, S. Q.; Boadi, E. O.; Li, J.; Pang, X. L.; He, J.; Chang, Y. X., Traditional herbal medicine: Therapeutic potential in rheumatoid arthritis. Journal of Ethnopharmacology 2021, 279, 114368.

[8] Vandewalle, J.; Luypaert, A.; De Bosscher, K.; Libert, C., Therapeutic mechanisms of glucocorticoids. Trends in Endocrinology and Metabolism 2018, 29 (1), 42-54.

[9] Weyand, C. M.; Goronzy, J. J., Immunometabolism in early and late stages of rheumatoid arthritis. Nature Reviews Rheumatology 2017, 13 (5), 1-11.

[10] Wójcik, P.; Gegotek, A.; Zarkovic, N.; Skrzydlewska, E., Oxidative stress and lipid mediators modulate immune cell functions in autoimmune diseases. International Journal of Molecular Sciences 2021, 22 (2), 22020723.

[11] Feng, L. J.; Jiang, T. C.; Zhou, C. Y.; Yu, C. L.; Shen, Y. J.; Li, J.; Shen, Y. X., Activated macrophage-like synoviocytes are resistant to endoplasmic reticulum stress-induced apoptosis in antigen-induced arthritis. Inflammation Research 2014, 63 (5), 335-346.

[12] Derksen, V.; Huizinga, T. W. J.; van der Woude, D., The role of autoantibodies in the pathophysiology of rheumatoid arthritis. Seminars in Immunopathology 2017, 39 (4), 437-446.

[13] Phull, A. R.; Nasir, B.; ul Haq, I.; Kim, S. J., Oxidative stress, consequences and ROS mediated cellular signaling in rheumatoid arthritis. Chemico-Biological Interactions 2018, 281, 121-136.

[14] Yang, Y. H.; Guo, L. N.; Wang, Z.; Liu, P.; Liu, X. J.; Ding, J. S.; Zhou, W. H., Targeted silver nanoparticles for rheumatoid arthritis therapy via macrophage apoptosis and Re-polarization. Biomaterials 2021, 264, 120390.

[15] Kalashnikova, I.; Chung, S.-J.; Nafiujjaman, M.; Hill, M. L.; Siziba, M. E.; Contag, C. H.; Kim, T., Ceria-based nanotheranostic agent for rheumatoid arthritis. Theranostics 2020, 10 (26), 11863-11880.

[16] Liu, J.; Zhao, Y.; Guo, Q.; Wang, Z.; Wang, H.; Yang, Y.; Huang, Y., TAT-modified nanosilver for combating multidrug-resistant cancer. Biomaterials 2012, 33 (26), 6155-6161.

[17] Xiu, Z.-m.; Zhang, Q.-b.; Puppala, H. L.; Colvin, V. L.; Alvarez, P. J. J., Negligible particle-specific antibacterial activity of silver nanoparticles. Nano Letters 2012, 12 (8), 4271-4275.

[18] Zhang, X.; Servos, M. R.; Liu, J., Fast pH-assisted functionalization of silver nanoparticles with monothiolated DNA. Chemical Communications 2012, 48 (81), 10114-10116.

[19] Li, F.; Yang, G.; Aguilar, Z. P.; Xiong, Y.; Xu, H., Affordable and simple method for separating and detecting ovarian cancer circulating tumor cells using BSA coated magnetic nanoprobes modified with folic acid. Sensors and Actuators B-Chemical 2018, 262, 611-618.

[20] Rollett, A.; Reiter, T.; Nogueira, P.; Cardinale, M.; Loureiro, A.; Gomes, A.; Cavaco-Paulo, A.; Moreira, A.; Carmo, A. M.; Guebitz, G. M., Folic acid-functionalized human serum albumin nanocapsules for targeted drug delivery to chronically activated macrophages. International Journal of Pharmaceutics 2012, 427 (2), 460-466.

[21] Zhang, Q.; Lin, S.; Shi, S.; Zhang, T.; Ma, Q.; Tian, T.; Zhou, T.; Cai, X.; Lin, Y., Anti-inflammatory and antioxidative effects of tetrahedral DNA nanostructures via the modulation of macrophage responses. Acs Applied Materials & Interfaces 2018, 10 (4), 3421-3430.

[22] Kim, J.; Kim, H. Y.; Song, S. Y.; Go, S.-h.; Sohn, H. S.; Baik, S.; Soh, M.; Kim, K.; Kim, D.; Kim, H.-C.; Lee, N.; Kim, B.-S.; Hyeon, T., Synergistic oxygen generation and reactive oxygen species scavenging by manganese ferrite/ceria co-decorated nanoparticles for rheumatoid arthritis Treatment. Acs Nano 2019, 13 (3), 3206-3217.